

The spectrum and flavor composition of the astrophysical neutrinos in IceCube

Atsushi Watanabe *

Maskawa Institute for Science and Culture, Kyoto Sangyo University, Kyoto 603-8555, Japan

(December, 2014)

Abstract

We fit the energy distribution of the IceCube starting events by a model which involves four parameters in the neutrino spectrum, namely three normalizations n_e, n_μ, n_τ and a common power-law index γ , with a fixed background simulated by IceCube. It is found that the best fit index is $\gamma = 2.7$ with $\chi^2_{\min} = 32.3/24$ dof. As for the two parameter model involving a democratic normalization and an index, the best fit is at $\gamma = 2.8$ with $\chi^2_{\min} = 33.9/26$ dof. The flavored model and the democratic model do not have much difference in the quality of the (energy-spectrum) fit. The standard 1 : 1 : 1 composition is not disfavored by the current data.

* watanabea@cc.kyoto-su.ac.jp

1 Introduction

IceCube has recently made a great success in the observation of the high-energy neutrinos of extraterrestrial origin. In their three years of data, 37 events have been found in 30 TeV–2 PeV energy range [1, 2, 3]. They have concluded that the hypothesis of the atmospheric neutrino origin is rejected at 5.7σ , heralding a new era of high-energy astronomy. The analysis with a lowered threshold down to 1 TeV also shows a significant contribution from the astrophysical component [4]. Neutrino sky which will be seen by the existing and the future neutrino telescopes will provide indispensable information to understand the origin of cosmic rays, physics of Gamma Ray Bursts, GZK processes, etc. Since the first announcement of the two PeV cascades, many authors have speculated about the sources of the observed high-energy neutrinos [5].

While the high-energy neutrinos are unique astronomical messengers, they may also play an interesting role in particle physics. Neutrino decay [6], pseudo-Dirac neutrinos [7], and Lorentz/CPT violation [8] have been discussed for long time as new physics testable by high-energy neutrinos. More recently, the isolated nature of the events around 1 PeV [3] have triggered a variety of intriguing ideas such as decay of long-lived particles [9], exotic mediators for neutrino absorbtions [10], new physics in the detection processes [11]. Obviously more data is needed to deal with such diverse hypotheses and speculations.

Flavor ratios for the three types of neutrinos are one of the key information for making further progress in these subjects [12]. One of the benchmark ratios for the source fluxes is $\Phi_e^0 : \Phi_\mu^0 : \Phi_\tau^0 = 1 : 2 : 0$. Lepton mixing changes this ratio to $\simeq 1 : 1 : 1$ at Earth [13]. Depending on astrophysical processes at the sources or new physics involved in the production, propagation and detection, the democratic composition at Earth may be significantly changed [12, 13].

In this paper, we study the flavor composition of high-energy neutrinos by using the three years data of IceCube [3]. Making the normalizations of power-law fluxes be flavor dependent, we fit the data and report the best fit and the intervals for the normalizations.

This issue was first addressed in Ref. [14], where they found that the $1 : 1 : 1$ composition at Earth with E_ν^{-2} spectrum is disfavored at 92% CL with the best fit composition $1 : 0 : 0$. They analyzed the total number of the shower and the track events which are integrated over the deposited energies. A goal of this paper is to study the impact of the energy distributions on the determination of the flavor ratios. We model the astrophysical neutrino fluxes for each flavor Φ_α ($\alpha = e, \mu, \tau$) as $\Phi_\alpha = n_\alpha E_\nu^{-\gamma}$, where n_α is the (flavor

dependent) normalization, E_ν is the neutrino energy, and γ is the spectral index. The model parameters to be determined are n_α and γ . By seeking the global minimum of a χ^2 function (see Section 3) with respect to these four parameters, we study the interplay between the flavor ratios and the spectral index. Our emphasis is, however, not on the numbers themselves given by the analysis, but on the qualitative differences between the flavored model and the usual democratic model, which may be highlighted by taking account of the energy distribution.

This paper is organized as follows. In Section 2, the calculations for the number of events by the astrophysical neutrinos are demonstrated. In Section 3, we discuss the method of the statistical analysis and show the results. Section 4 is for conclusions.

2 Number of events

2.1 Astrophysical neutrino events

Following Ref. [2, 3], we focus on the neutrino events whose vertices are contained in the detector volume (so-called “starting events”). The neutrinos leave their signals via neutrino–nucleon (νN) scattering. There are two main topologies of the neutrino events; the showers and the tracks. The electron neutrinos ν_e trigger the shower events by the charged current (CC) and the neutral current (NC) interactions. The muon neutrinos ν_μ produce both tracks and showers by the CC and NC interactions, respectively. The tau neutrinos ν_τ with the energies less than ~ 1 PeV produce showers by CC and NC, whereas ν_τ with energies greater than 1 PeV may produce distinct events called double-bang and lollipop [15]. In this paper, we assume ν_τ triggers only showers since we focus on the neutrino events whose energies are less than a few PeV*.

Let us first focus on the down-going events where the attenuation by Earth is irrelevant. The number of the shower events by the CC interactions of $\nu_e N$ and $\nu_\tau N$ are given by

$$\nu_{CC}^{\text{sh}} = 2\pi T N_A \int dE_\nu V_{CC}^{e,\tau} \sigma_{CC} \Phi_{e,\tau}, \quad (1)$$

where $T = 988$ days of exposure time, $N_A = 6.022 \times 10^{23} \text{ g}^{-1}$, E_ν is the neutrino energy, V_{CC}^e and V_{CC}^τ are the effective masses of the detector [2], σ_{CC} is the νN total cross section for the CC interactions [16], Φ_e and Φ_τ stand for the ν_e and ν_τ fluxes, respectively. The

*The taus produced from ν_τ -CC decay to muons in 17.4% branching ratio, and such events are classified as tracks. The inclusion of this track events slightly changes the following results on the flavor composition. However, the best fit values of the spectral index γ are not changed.

factor 2π accounts for the integration over Southern sky under the assumption that the neutrino fluxes are isotropic. In the CC channel of $\nu_e N$ and $\nu_\tau N$, almost all neutrino energy is converted to the electromagnetic deposited energy (E_{em}). In what follows, we assume $E_\nu = E_{\text{em}}$ for these CC processes.

The number of the shower events by the NC interactions of $\nu_\alpha N$ ($\alpha = e, \mu, \tau$) are given by

$$\nu_{\text{NC}}^{\text{sh}} = 2\pi T N_A \int_{E_0/\langle y \rangle}^{E_1/\langle y \rangle} dE_\nu V_{\text{NC}} \sigma_{\text{NC}} \Phi_\alpha, \quad (2)$$

where V_{NC} is the effective mass for the NC processes [2], σ_{NC} is the νN total cross section for the NC interactions [16], and $\langle y \rangle$ is the mean inelasticity, which is the mean energy fraction carried by the kicked quark in the final state [16]. The formula Eq. (2) shows the number of events for the shower energy between E_0 and E_1 .

Finally, the number of the track events by the CC interactions of $\nu_\mu N$ is given by

$$\nu^{\text{tr}} = 2\pi T N_A \int_{E_0/\langle y \rangle}^{E_1/\langle y \rangle} dE_\nu V_{\text{CC}}^\mu \sigma_{\text{CC}} \Phi_\mu, \quad (3)$$

where V_{CC}^μ is the effective mass for the ν_μ CC process [2]. The out-going muons produced inside the instrumental volume usually escape from the volume, such that the showers at the starting vertices dominantly contribute to the deposited energies. In this work, we assume the deposited energies are equal to the starting shower energies, and use Eq. (3) for the track events whose deposited energies between E_0 and E_1 .

For the up-going events (the events induced by the neutrinos coming from Northern sky), the events are calculated by Eq. (1), (2) and (3) with the replacement $(2\pi) \rightarrow (2\pi)S(E_\nu)$, where $S(E_\nu)$ is the shadow factor [16] varying from zero to unity, which accounts for the attenuation of the neutrinos by Earth. The calculations for the antineutrino are done by replacing the cross-sections which are slightly different from the ordinary ones [16].

2.2 Astrophysical neutrino fluxes

In this work, we consider isotropic diffuse fluxes for the astrophysical neutrinos. In order to make the model be sensitive to the neutrino flavors in a simple way, let the normalization of the astrophysical neutrino flux for each flavor be independent, while assuming the spectra follow a common power law;

$$\Phi_\alpha = n_\alpha E_\nu^{-\gamma}, \quad (\alpha = e, \mu, \tau). \quad (4)$$

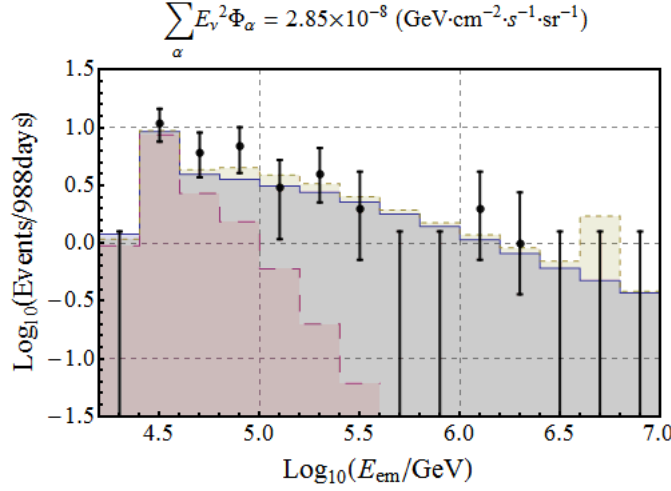


Figure 1: Deposited energy distribution of the astrophysical neutrino and the background events. The solid line shows the sum of the astrophysical neutrino events calculated by Eqs.(1)–(4) and the atmospheric background events (shown by the long-dashed line) simulated by the IceCube collaboration [3]. The short-dashed line is the IceCube estimation of the total events with $E^2\Phi = 0.95 \times 10^{-8} \text{ GeV cm}^{-1} \text{ s}^{-1} \text{ sr}^{-1}$ for each flavor. The black dots are the observed data.

Fig. 1 shows typical examples of the deposited energy distributions of the events. The solid line shows the summation of the astrophysical neutrino events calculated by Eqs.(1)–(4) and the background events (shown by the long-dashed line) simulated by the IceCube collaboration [3]. The IceCube estimation of the total events is also shown by the short-dashed line for comparison. The black dots are the observed data. In accordance with Ref. [3], the flux for each flavor is set as $n_{\alpha} = 0.95 \times 10^{-8} \text{ GeV cm}^{-1} \text{ s}^{-1} \text{ sr}^{-1}$ for $\alpha = e, \mu, \tau$ with $\gamma = 2.0$, and the neutrino/antineutrino ($\nu/\bar{\nu}$) fraction is taken to be unity. It is seen from Fig. 1 that the estimation by Eqs.(1)–(4) agrees well with the IceCube analysis, up to the large discrepancy at the bin for $E_{\text{em}} = 10^{6.6} - 10^{6.8} \text{ GeV}$. The shower and the track fraction of the astrophysical neutrino events are 82% and 18%, respectively. These numbers are also agree with Ref. [3].

The large discrepancy around $E_{\text{em}} = 10^{6.7} \text{ GeV}$ is due to the Glashow resonance [17], which is the resonant production of the W^- boson in $\bar{\nu}_e e$ scattering at $E_{\nu} = 6.3 \text{ PeV}$. This effect is not included in Fig. 1. The significance of this resonance strongly depends on the $\nu/\bar{\nu}$ fraction [18], which would be a nuisance to the current purpose. Since no events larger than $\sim 2 \text{ PeV}$ have been observed, we first avoid the uncertainty from the $\nu/\bar{\nu}$ fraction by assuming that the power-law fluxes have a cutoff at $E_{\nu} = 3.0 \text{ PeV}$. In this

case, the $\nu/\bar{\nu}$ fraction does not make much difference on the result of the following flavor analysis. The effect of the Glashow resonance on the fluxes without cutoff is discussed later (see Table 2 and the related text). In what follows, we set the $\nu/\bar{\nu}$ ratio to be unity as a typical example. Such a ratio is realized if the neutrinos are produced on source by the proton-proton scattering.

3 Flavor compositions

We assume that the shower and track events are Poisson distributed around mean values μ^{sh} and μ^{tr} . The observed data is fitted by minimizing the logarithm of the likelihood ratio of the current model to the saturated model [19]

$$\chi^2 = \chi_{\text{shower}}^2 + \chi_{\text{track}}^2, \quad (5)$$

$$\chi_{\text{shower}}^2 = 2 \sum_{i=1}^{14} \left(\mu_i^{\text{sh}} - N_i^{\text{sh}} + N_i^{\text{sh}} \ln \frac{N_i^{\text{sh}}}{\mu_i^{\text{sh}}} \right), \quad (6)$$

where i labels the energy bins (see in Fig. 1), N^{sh} is the observed shower events [3]. The mean of the shower events μ^{sh} is given by

$$\mu^{\text{sh}} = \nu^{\text{sh}} + b^{\text{sh}}, \quad (7)$$

where ν^{sh} stands for $\nu_{\text{CC}}^{\text{sh}} + \nu_{\text{NC}}^{\text{sh}}$ summed over the up and down-going, the neutrino and antineutrino components. b^{sh} is the background shower events. The symbols with the subscript i stand for the values for the i -th bin. The function χ_{track}^2 is defined in the same manner as χ_{shower}^2 .

For the background estimations of b^{sh} and b^{tr} , we use the numbers in Ref. [3]; the binned expected numbers for “atmospheric neutrino (π/K)” and “muon flux” shown in Fig. 2 of Ref. [3]. In order to breakdown the atmospheric neutrino events into the showers and the tracks, we assume that the atmospheric neutrino events are solely induced by ν_{μ} and its CC and NC reactions are identified as the tracks and the showers, respectively. This estimates that the track events account for 76% of the atmospheric neutrino events in each energy bin[†].

[†]A more realistic number given in Ref. [3] is 69%. If we use this number in the following analysis, the best fit values of γ and n_{α} are accordingly changed by a few percent.

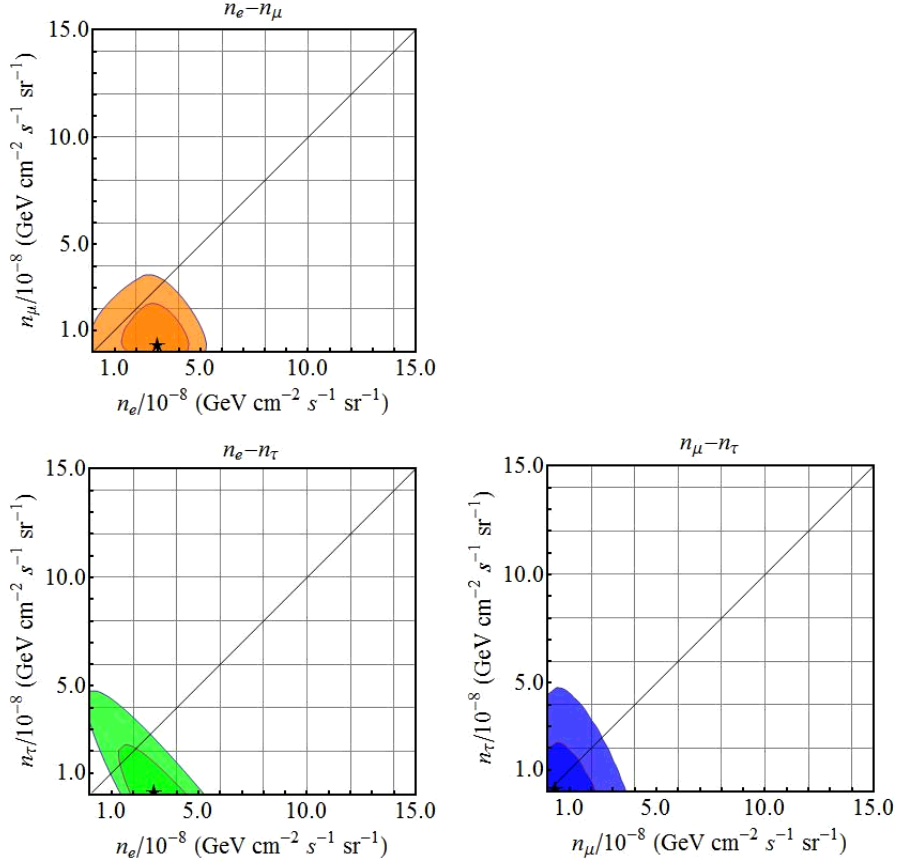


Figure 2: Best fit and intervals of n_e, n_μ, n_τ in the case of E_ν^{-2} spectrum ($\gamma = 2.0$). The three panels show the regions in the three dimensional (n_e, n_μ, n_τ) space projected to the two dimensional planes. The symbol \star stands for the best fit, and the inner (outer) region filled dark (light) is the 68% (95%) region.

For a fixed value of the spectral index γ , the best fit of n_e, n_μ, n_τ is given by the minimum of Eq. (5). In addition to the best fit, we report the regions which satisfy $\chi^2 < \chi_{\min}^2 + 3.53$ (7.82) as approximate 68% (95%) confidence regions [19].

Fig. 2 shows the best fit and the intervals in the case of E_ν^{-2} spectrum ($\gamma = 2.0$). The three panels show the projections of the regions in the three dimensional (n_e, n_μ, n_τ) space. The symbol \star stands for the best fit, and the inner (outer) region filled in dark (light) colors is the 68% (95%) region. The best fit is $n_e = 3.0 \times 10^{-8}$, $n_\mu = 3.9 \times 10^{-9}$, $n_\tau = 0$ in the unit of $\text{GeV cm}^{-1} \text{s}^{-1} \text{sr}^{-1}$ where $\chi_{\min}^2 = 42.7/25 \text{ dof}$. Starting from the minimum, the χ^2 function is well increasing along the n_e axis, whereas it sharply stands up only toward the increasing direction along the n_μ and n_τ axes. Although the best fit of n_μ is not zero, the increasing of χ^2 is moderate along the decreasing n_μ direction.

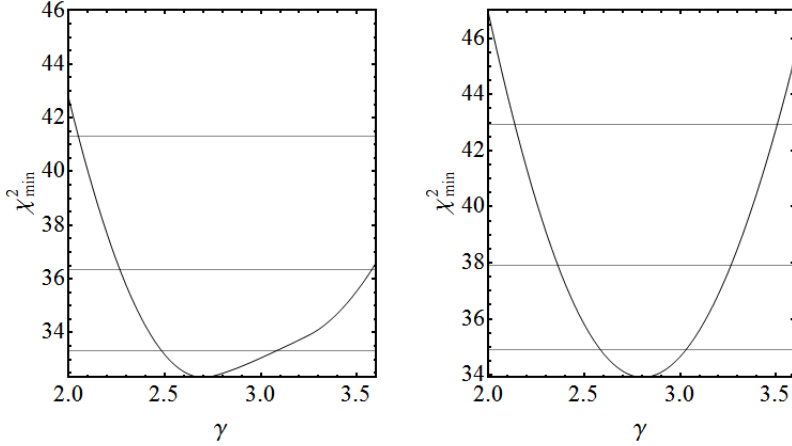


Figure 3: Minimum of χ^2 (Eq. (5)) for each value of the spectral index γ . The left panel shows the case where n_e , n_μ and n_τ are independent, while the right panel shows the case where the condition $n_e = n_\mu = n_\tau$ is imposed. The horizontal lines show the minimum + 1, 4, and 9, as the references for the 1,2 and 3 σ ranges of γ .

The standard $\Phi_e : \Phi_\mu : \Phi_\tau = 1 : 1 : 1$ hypothesis is represented by the $n_e = n_\mu = n_\tau$ trajectory in the (n_e, n_μ, n_τ) space. It is seen from Fig. 2 that 1 : 1 : 1 is lying on outside of the 68% region. The minimum of χ^2 along the $n_e = n_\mu = n_\tau$ trajectory is $\chi^2_{\min}|_{n_e=n_\mu=n_\tau} = 46.9/27$ dof, which means the $n_e = n_\mu = n_\tau$ trajectory is tangent to the 76% surface in the (n_e, n_μ, n_τ) space. If we change the background assumption by replacing the track fraction 76% with 69%(50%), $\chi^2_{\min}|_{n_e=n_\mu=n_\tau}$ goes down from 46.9 to 44.5(39.0).

The minimum of the flavored model with E_ν^{-2} spectrum is $\chi^2_{\min} = 42.7/25$ dof, which means that this fit must be also poor. Better fits are obtained with the larger values of γ . Fig. 3 shows the minimum of χ^2 (Eq. (5)) for each value of the spectral index γ . The left panel shows the case where n_e , n_μ and n_τ are independent, while the right panel shows the case where the condition $n_e = n_\mu = n_\tau$ is imposed. The left panel tells us that the global minimum is away from $\gamma = 2.0$. The minimum is achieved at $\gamma = 2.7$, where $\chi^2_{\min} = 32.3/24$ dof, which is more acceptable than $\gamma = 2.0$. In the right panel of Fig. 3, $\chi^2_{\min} = 33.9/26$ dof at $\gamma = 2.8$. When we omit the events below ~ 60 TeV and perform a fit without the lower three bins, the best fit index becomes $\gamma = 2.3$ for the flavored model and $\gamma = 2.4$ for the democratic model, in agreement with Ref. [3].

Fig. 4 shows the regions for the normalization constants in the case of $\gamma = 2.7$. In the

	$\gamma = 2.0$		$\gamma = 2.7$	
	68%	95%	68%	95%
T	0 - 0.47	0 - 0.63	0 - 0.53	0 - 0.70
R	0.62 - ∞	0 - ∞	0 - ∞	0 - ∞

Table 1: Crude intervals for the flux ratios $T = \Phi_\mu/(\Phi_e + \Phi_\mu + \Phi_\tau)$ and $R = \Phi_e/\Phi_\tau$. In each column for $\gamma = 2.0$ and $\gamma = 2.7$, the left (right) item shows the interval corresponding to the 68% (95%) region presented in Fig. 2 and Fig. 4.

plots, the normalization parameters are taken as

$$E_\nu^2 \Phi_\alpha = n_\alpha \left(\frac{E_\nu}{10^5 \text{ GeV}} \right)^{-0.7}, \quad (\alpha = e, \mu, \tau). \quad (8)$$

The best fit is $n_e = 4.9 \times 10^{-8}$, $n_\mu = 5.8 \times 10^{-9}$, $n_\tau = 0$ in the unit of $\text{GeV cm}^{-1} \text{s}^{-1} \text{sr}^{-1}$. Compared with $\gamma = 2.0$ (Fig. 2), wider ranges are allowed for $\gamma = 2.7$. The $n_e = n_\mu = n_\tau$ trajectory is tangent to the 38% surface, which means the 1 : 1 : 1 ratio is consistent with the current observation.

Note in passing that we are able to put the intervals on the flux ratios frequently quoted in literature. The two ratios $T \equiv \Phi_\mu/(\Phi_e + \Phi_\mu + \Phi_\tau)$ and $R \equiv \Phi_e/\Phi_\tau$ are often discussed [13]. As a crude estimate of the confidence intervals, we show in Table. 1 the ranges of the functions T and R under the domain of the 68%(95%) regions of (n_e, n_μ, n_τ) (the space defined by $\chi^2 \leq \chi_{\min}^2 + 3.53$ (7.82)). Notice that this does not take into account the cancellation of the uncertainties, so that the actual intervals may be narrower than shown here.

Finally, we comment on the effects of the Glashow resonance and the misidentification (mis-ID) of the track events. It is pointed out that 30% of the track events could be misidentified as showers [20], and this effect has strong impacts on the determination of the flavor composition [21]. In fact, we find that both of these effects have moderate impacts on the quality of the fit, but they significantly change the best fit of the flavor ratio and the exclusion level of 1 : 1 : 1 in each model.

The results are summarized in Table 2. As is expected, the inclusion of mis-ID allows larger fractions of ν_μ and reduces the exclusion level of 1 : 1 : 1. In the flavored model with the four parameters (γ, n_α) being floated, the best fit ratio 1 : 0.1 : 0 is changed to 1 : 0.2 : 0, and the exclusion limit 38% goes down to 12%. The best fit value of γ is not changed by the mis-ID effects.

On the other hand, the effect of the Glashow resonance shifts the best fit of γ to a

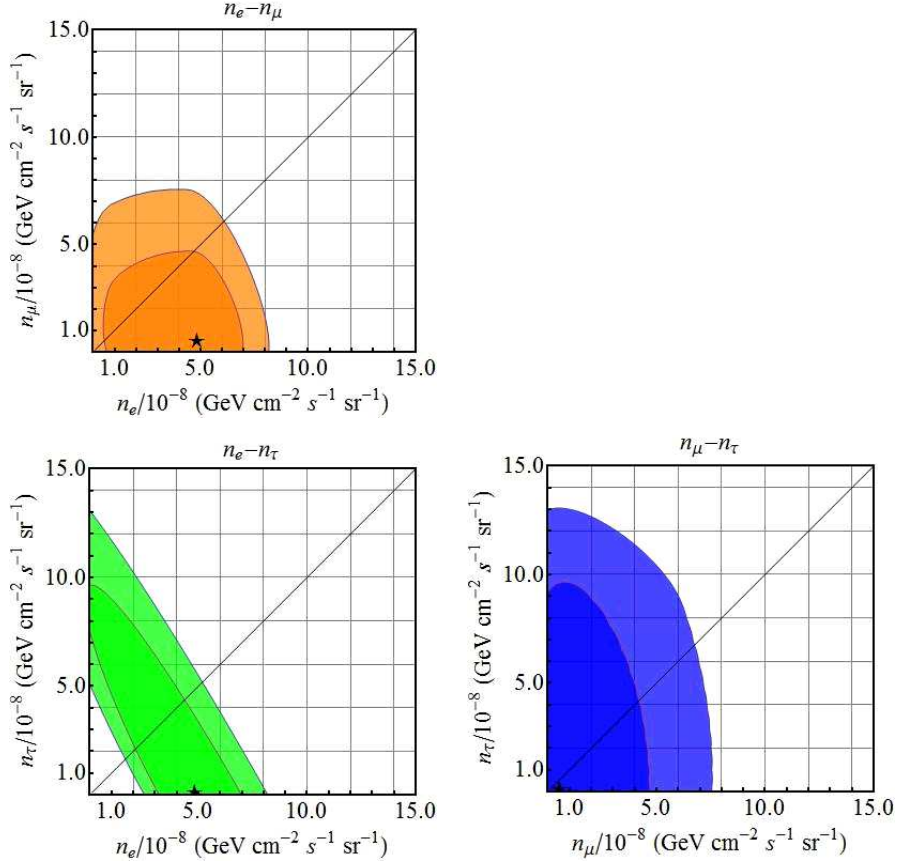


Figure 4: The same plots as in Fig. 2, but for $E_\nu^{-2.7}$ spectrum ($\gamma = 2.7$).

slightly softer value, mitigating the conflict between the null observation and the enhanced event rate at the resonance bin. A striking change is the pushing-up of the ν_τ component at the best fit. There are two reasons for this increasing of ν_τ . The first reason is the difference of the detection efficiencies of ν_e and ν_τ at the lower energies. According to Ref. [2], the effective volume of ν_e is as twice as large as ν_τ around 40-100 TeV. As the spectrum gets soft, the events less than ~ 100 TeV get too large, so that ν_τ is preferred for its lower detection rate than ν_e . In fact, in the search of the best fit ratio, ν_τ becomes dominant over ν_e for $\gamma \gtrsim 2.8$ in any flavored model. The second reason is that ν_τ can account for the shower events while keeping the resonance event suppressed. This effect may slightly push down the value of γ at which ν_τ overcomes ν_e . Since the inclusion of the Glashow resonance favors softer spectra, the best fit of the ν_τ fraction accordingly increases due to the first reason mentioned above.

Model	Best fit	χ^2_{\min}	Exclusion level of 1:1:1
(γ, n_α) -free (4P)	$\gamma = 2.7$ 1 : 0.1 : 0	$\chi^2_{\min} = 32.3/24$ dof	38%
mis-ID	$\gamma = 2.7$ 1 : 0.2 : 0	$\chi^2_{\min} = 32.2/24$ dof	12%
GR	$\gamma = 2.9$ 1 : 0.1 : 0.7	$\chi^2_{\min} = 32.9/24$ dof	27%
mis-ID+GR	$\gamma = 2.8$ 1 : 0.4 : 0.7	$\chi^2_{\min} = 32.8/24$ dof	10%
$\gamma = 2.0, n_\alpha$ -free (3P)	1 : 0.1 : 0	$\chi^2_{\min} = 42.7/25$ dof	76%
mis-ID	1 : 0.4 : 0	$\chi^2_{\min} = 42.2/25$ dof	47%
GR	1 : 0.2 : 0.8	$\chi^2_{\min} = 54.1/25$ dof	32%
(γ, n) -free (2P)	$\gamma = 2.8$	$\chi^2_{\min} = 33.9/26$ dof	-
mis-ID	$\gamma = 2.8$	$\chi^2_{\min} = 32.8/26$ dof	-

Table 2: Summary of the best fit, χ^2_{\min} , and the Feldman-Cousins exclusion level [22] of 1 : 1 : 1. “ (γ, n_α) -free (4P)” stands for the model where the four parameters $\gamma, n_e, n_\mu, n_\tau$ are floated. “ $\gamma = 2.0, n_\alpha$ -free (3P)” is the model where three parameters n_e, n_μ, n_τ are free with the fixed index $\gamma = 2.0$. The third model “ (γ, n) -free (2P)” is the case where γ and the normalization $n = n_e = n_\mu = n_\tau$ are varied. The sub-items “mis-ID”, “GR”, and “mis-ID+GR” show the options that include the effect of the 30% misidentification of the tracks as showers, the Glashow Resonance without the energy cutoff, and the combination of both, respectively. In the column of “Best fit”, the ratios shows 1 : n_μ/n_e : n_τ/n_e at the best fit values of the normalizations.

4 Conclusions

The current data of the IceCube’s starting events seemingly shows a paucity of the muon events. Above 30 TeV, just eight tracks have been observed against the background of 8.4 ± 4.2 cosmic ray muon events and $6.6^{+5.9}_{-1.6}$ atmospheric neutrino events. If this tendency would hold, it suggests that the standard 1 : 1 : 1 scenarios should be revised, and may even indicate the existence of some new physics.

In this work, we have studied the flavor composition of the astrophysical neutrinos observed in IceCube, especially focusing on the impact of the spectral index γ . Our point is not to give a precise estimation for the best fit and the intervals of the relevant parameters, but to illustrate important qualitative features in the flavor and the spectrum

analysis of the astrophysical neutrinos. For this purpose, we consider the model with the three-flavor normalizations n_e, n_μ, n_τ and a common index γ kept independent (the flavored model), and compare it to the usual model with a common normalization and an index (the democratic model).

It is found that the global minimum of the flavored model is at $\gamma = 2.7$ with $\chi^2_{\min} = 32.3/24$ dof. As for the democratic model, the best fit is at $\gamma = 2.8$ with $\chi^2_{\min} = 33.9/26$ dof. The democratic model and the flavored model do not have much difference in the quality of the (energy-spectrum) fit. The standard $1 : 1 : 1$ composition is consistent with the current data.

However, the flavor composition may affect the interval determination of γ . The left panel of Fig. 3 shows that the χ^2 does not quickly stand up as γ increases, indicating that the determination of γ might be more challenging for the flavored model than for the democratic case. The current background model does not leave much room for the track contributions from the astrophysical neutrinos at lower energies. Thus the $1 : 1 : 1$ case gets trouble at the lower energy bins as γ becomes large, whereas the flavored model can avoid the conflict by taking the configuration where the muon component is suppressed. The inference of the spectral index may become a nontrivial task once the flavor degrees of freedom are switched on.

Acknowledgments

I thank Werner Rodejohann for his contribution in the early stage of this work. I also thank Thomas Schwetz and Hiroaki Sugiyama for useful discussions on statistics.

References

- [1] M. G. Aartsen *et al.* [IceCube Collaboration], Phys. Rev. Lett. **111** (2013) 021103 [arXiv:1304.5356 [astro-ph.HE]].
- [2] M. G. Aartsen *et al.* [IceCube Collaboration], Science **342** (2013) 1242856 [arXiv:1311.5238 [astro-ph.HE]].
- [3] M. G. Aartsen *et al.* [IceCube Collaboration], Phys. Rev. Lett. **113** (2014) 101101 [arXiv:1405.5303 [astro-ph.HE]].
- [4] M. G. Aartsen *et al.* [IceCube Collaboration], arXiv:1410.1749 [astro-ph.HE].

- [5] I. Cholis and D. Hooper, JCAP **1306** (2013) 030 [arXiv:1211.1974 [astro-ph.HE]]; O. E. Kalashev, A. Kusenko and W. Essey, Phys. Rev. Lett. **111** (2013) 4, 041103 [arXiv:1303.0300 [astro-ph.HE]]; D. B. Fox, K. Kashiyama and P. Me'szaro's, Astrophys. J. **774** (2013) 74 [arXiv:1305.6606 [astro-ph.HE]]; F. W. Stecker, Phys. Rev. D **88** (2013) 4, 047301 [arXiv:1305.7404 [astro-ph.HE]]; K. Murase and K. Ioka, Phys. Rev. Lett. **111** (2013) 12, 121102 [arXiv:1306.2274 [astro-ph.HE]]; R. Laha, J. F. Beacom, B. Dasgupta, S. Horiuchi and K. Murase, Phys. Rev. D **88** (2013) 043009 [arXiv:1306.2309 [astro-ph.HE]]; H. Gao, B. Zhang, X. F. Wu and Z. G. Dai, Phys. Rev. D **88** (2013) 043010 [arXiv:1306.3006 [astro-ph.HE]]; K. Murase, M. Ahlers and B. C. Lacki, Phys. Rev. D **88** (2013) 12, 121301 [arXiv:1306.3417 [astro-ph.HE]]; L. A. Anchordoqui, H. Goldberg, M. H. Lynch, A. V. Olinto, T. C. Paul and T. J. Weiler, Phys. Rev. D **89** (2014) 8, 083003 [arXiv:1306.5021 [astro-ph.HE]]; S. Razzaque, Phys. Rev. D **88** (2013) 10, 103003 [arXiv:1307.7596 [astro-ph.HE]]; M. Ahlers and K. Murase, Phys. Rev. D **90**, no. 2, 023010 (2014) [arXiv:1309.4077 [astro-ph.HE]]; N. Fraija, Mon. Not. Roy. Astron. Soc. **437** (2014) 2187 [arXiv:1310.7061 [astro-ph.HE]]; A. M. Taylor, S. Gabici and F. Aharonian, Phys. Rev. D **89** (2014) 10, 103003 [arXiv:1403.3206 [astro-ph.HE]]; M. Ahlers and F. Halzen, Phys. Rev. D **90** (2014) 043005 [arXiv:1406.2160 [astro-ph.HE]]; J. Becker Tjus, B. Eichmann, F. Halzen, A. Kheirandish and S. M. Saba, Phys. Rev. D **89** (2014) 12, 123005 [arXiv:1406.0506 [astro-ph.HE]]; A. Bhattacharya, R. Enberg, M. H. Reno and I. Sarcevic, arXiv:1407.2985 [astro-ph.HE]; W. Winter, Phys. Rev. D **90** (2014) 10, 103003 [arXiv:1407.7536 [astro-ph.HE]]; C. Y. Chen, P. S. B. Dev and A. Soni, arXiv:1411.5658 [hep-ph].
- [6] J. F. Beacom, N. F. Bell, D. Hooper, S. Pakvasa and T. J. Weiler, Phys. Rev. Lett. **90** (2003) 181301 [hep-ph/0211305].
- [7] S. T. Petcov, Phys. Lett. B **110** (1982) 245; M. Kobayashi, C. S. Lim and M. M. Nojiri, Phys. Rev. Lett. **67** (1991) 1685.
- [8] V. A. Kostelecky and M. Mewes, Phys. Rev. D **69** (2004) 016005 [hep-ph/0309025]; G. Barenboim and C. Quigg, Phys. Rev. D **67** (2003) 073024 [hep-ph/0301220].
- [9] B. Feldstein, A. Kusenko, S. Matsumoto and T. T. Yanagida, Phys. Rev. D **88** (2013) 1, 015004 [arXiv:1303.7320 [hep-ph]]; A. Esmaili and P. D. Serpico, JCAP **1311** (2013) 054 [arXiv:1308.1105 [hep-ph]]; T. Higaki, R. Kitano and R. Sato, JHEP **1407**

- (2014) 044 [arXiv:1405.0013 [hep-ph]]; A. Bhattacharya, R. Gandhi and A. Gupta, arXiv:1407.3280 [hep-ph]; Y. Ema, R. Jinno and T. Moroi, JHEP **1410** (2014) 150 [arXiv:1408.1745 [hep-ph]]; A. Esmaili, S. K. Kang and P. D. Serpico, arXiv:1410.5979 [hep-ph]; C. S. Fong, H. Minakata, B. Panes and R. Z. Funchal, arXiv:1411.5318 [hep-ph]; E. Dudas, Y. Mambrini and K. Olive, arXiv:1412.3459 [hep-ph].
- [10] K. Ioka and K. Murase, PTEP **2014** (2014) 6, 061E01 [arXiv:1404.2279 [astro-ph.HE]]; M. Ibe and K. Kaneta, Phys. Rev. D **90** (2014) 5, 053011 [arXiv:1407.2848 [hep-ph]]; K. Blum, A. Hook and K. Murase, arXiv:1408.3799 [hep-ph]; T. Araki, F. Kaneko, Y. Konishi, T. Ota, J. Sato and T. Shimomura, arXiv:1409.4180 [hep-ph].
- [11] A. N. Akay, O. Cakir, Y. O. Gunaydin, U. Kaya, M. Sahin and S. Sultansoy, arXiv:1409.5896 [hep-ph]; J. I. Illana, M. Masip and D. Meloni, arXiv:1410.3208 [hep-ph];
- [12] J. F. Beacom, N. F. Bell, D. Hooper, S. Pakvasa and T. J. Weiler, Phys. Rev. D **68** (2003) 093005 [Erratum-ibid. D **72** (2005) 019901] [hep-ph/0307025].
- [13] W. Rodejohann, JCAP **0701** (2007) 029 [hep-ph/0612047]; S. Pakvasa, W. Rodejohann and T. J. Weiler, JHEP **0802** (2008) 005 [arXiv:0711.4517 [hep-ph]]; S. Choubey and W. Rodejohann, Phys. Rev. D **80** (2009) 113006 [arXiv:0909.1219 [hep-ph]]; D. Meloni and T. Ohlsson, Phys. Rev. D **86** (2012) 067701 [arXiv:1206.6886 [hep-ph]]; F. Vissani, G. Pagliaroli and F. L. Villante, JCAP **1309** (2013) 017 [arXiv:1306.0211 [astro-ph.HE]]; X. J. Xu, H. J. He and W. Rodejohann, JCAP **12** (2014) 039 [arXiv:1407.3736 [hep-ph]].
- [14] O. Mena, S. Palomares-Ruiz and A. C. Vincent, Phys. Rev. Lett. **113** (2014) 9, 091103 [arXiv:1404.0017 [astro-ph.HE]]; S. Palomares-Ruiz, O. Mena and A. C. Vincent, arXiv:1411.2998 [astro-ph.HE].
- [15] J. G. Learned and S. Pakvasa, Astropart. Phys. **3** (1995) 267 [hep-ph/9405296, hep-ph/9408296].
- [16] R. Gandhi, C. Quigg, M. H. Reno and I. Sarcevic, Astropart. Phys. **5** (1996) 81 [hep-ph/9512364]; R. Gandhi, C. Quigg, M. H. Reno and I. Sarcevic, Phys. Rev. D **58** (1998) 093009 [hep-ph/9807264].

- [17] S. L. Glashow, Phys. Rev. **118** (1960) 316.
- [18] L. A. Anchordoqui, H. Goldberg, F. Halzen and T. J. Weiler, Phys. Lett. B **621** (2005) 18 [hep-ph/0410003]; A. Bhattacharya, R. Gandhi, W. Rodejohann and A. Watanabe, JCAP **1110** (2011) 017 [arXiv:1108.3163 [astro-ph.HE]]; V. Barger, L. Fu, J. G. Learned, D. Marfatia, S. Pakvasa and T. J. Weiler, Phys. Rev. D **90** (2014) 121301 [arXiv:1407.3255 [astro-ph.HE]].
- [19] K. A. Olive *et al.* [Particle Data Group Collaboration], Chin. Phys. C **38** (2014) 090001.
- [20] M. G. Aartsen *et al.* [IceCube Collaboration], arXiv:1502.03376 [astro-ph.HE].
- [21] S. Palomares-Ruiz, A. C. Vincent and O. Mena, arXiv:1502.02649 [astro-ph.HE].
- [22] G. J. Feldman and R. D. Cousins, Phys. Rev. D **57** (1998) 3873 [physics/9711021 [physics.data-an]].